# Thermodynamic modelling of reciprocating and Wankel type compressor for household refrigerators

Konrad Klotsche
*TU Dresden, Germany*, konrad.klotsche@tu-dresden.de

Thomas W. Moesch
*Institut fuer Energietechnik Bitzer-Stiftungsprofessur fuer Kaelte-, Kryo- und Kompressorentechnik, Technische Universität Dresden, Germany*, thomas.moesch@tu-dresden.de

Gotthard Will
*Technische Universität Dresden, Germany*

Ullrich Hesse
ullrich.hesse@tu-dresden.de

# Thermodynamic modelling of reciprocating and Wankel type compressor for household refrigerators

Konrad KLOTSCHE*, Thomas Werner MOESCH, Gotthard WILL, Ullrich HESSE

Technische Universität Dresden, Institute of Power Engineering,
Bitzer Chair of Refrigeration, Cryogenics and Compressor Technology,
Dresden, Germany
konrad.klotsche@tu-dresden.de

* Corresponding Author

## ABSTRACT

Recent studies point out various benefits of trochoid-type compressors in vapor compression heat pump cycles and air compression applications. However, the field of small household refrigeration is still dominated by reciprocating compressors. This study comparatively investigates the thermodynamic behavior of a reciprocating and Wankel-type compressor in household refrigerators using the compressor simulation software KVA, which has been developed at the TU Dresden. The results of the KVA calculations are compared to available experimental data of a typical household refrigeration compressor. The comparative investigation reveals the differences between both compressor types regarding internal losses such as flow losses and internal leakages and further phenomena. The results show that Wankel compressors are currently not competitive in domestic refrigeration applications.

## 1. INTRODUCTION

First trochoid-type compressor applications for refrigeration, automotive air conditioning and heat pumps were investigated in the 1970s/80s. Ogura (1982) introduced an automotive air conditioning 2:3 Wankel compressor. Kaiser and Kruse (1984) experimentally and analytically investigated different automotive AC compressor types and concluded that the tested 2:3 Wankel compressor was inferior due to the poor volumetric efficiency and a severe suction gas overheating. Wrede and Kruse (1986) analytically investigated both 1:2 and 2:3 trochoid compressor designs for heat pump applications: They found the 1:2 version to be more energy efficient due to smaller clearance ratio. Recent publications indicate further applications of Wankel machines. Wu et al. (2010) show the applicability of Wankel compressors in miniature-scale refrigeration systems. Antonelli et al. (2017) introduced a prototype Wankel expander for compressed air and saturated steam. Garside (2017) introduced a new Wankel design for air compression and vacuum production and suggests that the new Wankel design leads to a low clearance volume, low frictional losses, low vibrations, and more compact compressors. This meets some of the main criteria for household refrigerator compressors. However, the application of Wankel compressors in refrigerators has not been fully investigated yet and the refrigerator market is still dominated by hermetic reciprocating compressors. The authors therefor investigate a 2:3 Wankel design for R600a household refrigerators.

Experimental investigations are typically very time consuming and costly. The authors choose a theoretical approach and use the calculation software KVA which has been successfully applied on process gas compressors by Hesse and Will (2014). KVA is based on a 1-D thermodynamic model that includes interactions of the different chambers, valves and orifices all relevant compressor components focusing the thermodynamic behavior of the refrigerant. The applicability of the software is tested by analyzing the hermetic reciprocating compressor HTK55AA as used by Lang (2010) and comparing the calculation results to their experimental data. KVA is then applied on the Wankel geometry. The results lead to a better understanding of the increased thermodynamic losses compared to reciprocating compressors. The results indicate possible design limitations and improvements for future Wankel compressor designs.

## 2. KVA - ANALYSIS TOOL FOR COMPRESSOR SYSTEMS

The analysis tool for compressor systems KVA (in German: "**K**olben**v**erdichter**a**nlagen") is a development of the Bitzer Chair of Refrigeration, Cryogenics and Compressor Technology. The tool was originally developed for process gas compressors with a significantly higher compression power range as compared to household refrigeration applications. The analysis of such a compressor with KVA is therefore also a test of the quality and accuracy that can be achieved for smaller compressors.

The calculation procedure is based on a network model with each relevant gas-filled volume and flowed-through volume as one node. This includes all working chambers, the suction and pressure chambers and other volumes (buffer tanks, mufflers, crankcase, etc.) that are relevant to the compressor's thermodynamic behavior. In this analysis all thermodynamically relevant volumes were considered since a more complete simulation leads to a more precise calculation. All properties of these volumes (*V, m, T, p, h, s, e*) are time-dependent and location-independent within each volume. The volumes are interconnected by links which may represent pipes, valves and sealings. They are gas-filled elements which are mostly characterized by the flow through them. Volume boundaries are represented by wall elements in KVA. They represent the compressor component structure and allow a consideration of heat transfer between the gas and the compressor components. The heat conduction between adjacent wall elements may also be included.

All KVA calculations are based on the general gas equation and the first law of thermodynamics. The explicit formulation for the time-dependent behavior of the pressure and temperature within each gas volume is given by Equations (1) and (2).

$$\frac{1}{p}\frac{dp}{dt} = \frac{K}{K-1}\left(\frac{p}{m\,K\,R\,T}\frac{dQ}{dt} - \frac{1}{V}\frac{dV}{dt} - \frac{1}{K}\frac{dK}{dt}\right) \tag{1}$$

$$\frac{1}{T}\frac{dT}{dt} = \frac{K}{K-1}\left(\frac{p}{m\,K\,R\,T}\frac{dQ}{dt} - \frac{1}{V\,K}\frac{dV}{dt} - \frac{1}{K}\frac{dK}{dt}\right) - \frac{1}{m}\frac{dm}{dt} - \frac{1}{R}\frac{dR}{dt} \tag{2}$$

The parameter $K$ is defined as $K = h\,R^{-1}\,T^{-1}$. The change of heat over time $dQ/dt$ for each volume accounts for all heat flows and enthalpy flows across the volume boundaries. The governing equation for the law of mass conservation is $dm/dt = \sum \dot{m}_j$ which takes into account every mass flow $\dot{m}_j$ across the volume boundaries. The thermodynamic state over time is calculated by a time-step method over several crankshaft turns which uses a step size typically between $\Delta\varphi = 0.01° \ldots 1.0°$. The flow through the valves is calculated with a general nozzle flow approach (see for example Surek and Stempin (2014)) given by Equation (3).

$$\dot{m} = h_{\mathrm{v}}\, l_{\mathrm{v}}\, \alpha_{\mathrm{flow}}\, \psi_{\mathrm{f}} \sqrt{2\, p\, \varrho} \tag{3}$$

The valve (*e.g.* lamella, ring plate, poppets or similar elements) movement is based on the acting forces. The heat transfer between the gas volumes and the surrounding walls is characterized by heat transfer coefficients (HTC). The HTC are calculated using a general Nusselt number approach $Nu = f(Pr, Re)$ based on the Prandtl number $Pr$ and the Reynolds number $Re$. The latter considers the piston speed and the equivalent speed for the kinetic energy of the gas. This approach for the HTCs has shown a good agreement of experimental and simulation results of an air compressor in Hesse and Will (2014) where further information of the working principles of KVA is also provided.

## 3. MODELLING AND CALCULATION OF A RECIPROCATING COMPRESSOR

### 3.1 KVA model for a household refrigeration reciprocating compressor

The model of the reciprocating refrigerator compressor is based on the compressor data of Lang (2010). Lang investigated the compressor model ACC HTK 55 AA and published meaningful measurement results with information on the relevant experimental boundary conditions. Figure 1 shows views of the compressor with its relevant geometric data.

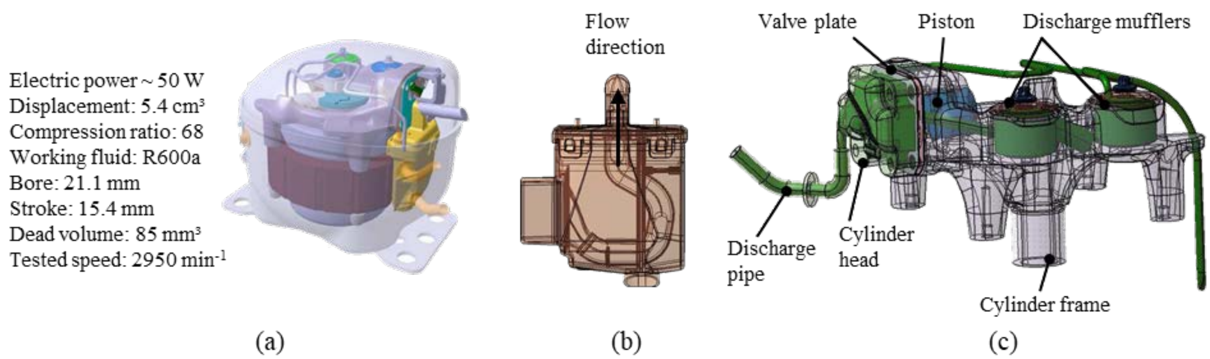


**Figure 1**: CAD view of ACC HTK55 AA with relevant compressor data (a), the suction muffler (b), and the high-pressure flow system (c)

The ACC HTK55 AA is a hermetic compressor with a suction port at the housing and a suction muffler prior to the working chamber. The length of the suction line is only a few centimeters and the suction line is connected to the inner compressor housing. The compressor housing is therefore filled with refrigerant at suction pressure level. The refrigerant flow into and out of the compression chamber is controlled by a self-acting reed valve at the inlet and at the outlet of the working chamber, respectively. The discharge line comprises three consecutive pulsation dampers, which are connected by short pipes.

The compressor structure, the internal flow path and all relevant geometric data were considered for the corresponding KVA compressor model as shown in Figure 2. The goal of the model is a reduction of the modelling effort while considering all essential compressor elements. This paper focusses on the modeling of the gas flow path. It consists of the suction line (*SL*) and a connected suction chamber (SC) which represents the suction side muffler. The next volume is the working chamber (WC) which is connected to SC by the suction valve (*SV*) at its inlet and to the discharge chamber (DC) by the discharge valve (*DV*) at its outlet. The discharge chamber (DC) is then connected to the pressure line (*DL*). The boundary conditions at the low-pressure inlet (L) and the high-pressure outlet (H) of the compressor were specified in accordance to the experiments of Lang (2010). The compressor housing is modelled by an upper and lower crankcase volume with a shell that is thermally coupled to the environment and the flow path elements. This allows a consideration of the heat transfer inside the compressor and the heat transfer to the environment. The valve parameters were estimated based on the geometrical and mechanical properties given by Lang (2010).

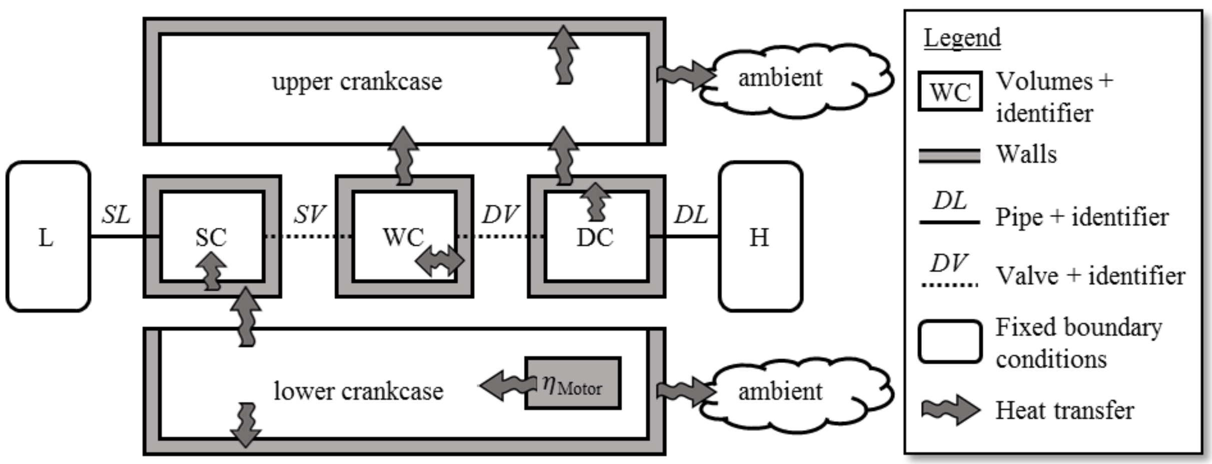


**Figure 2:** KVA model of the compressor ACC HTK55 AA

## 3.2 Comparison of experimental and KVA calculation results for the reciprocating compressor

The experimental results of Lang (2010) were selected as a suitable reference for the KVA calculation results. The comparison is based on the $p,V$ diagram that is shown in Figure 3 (a).

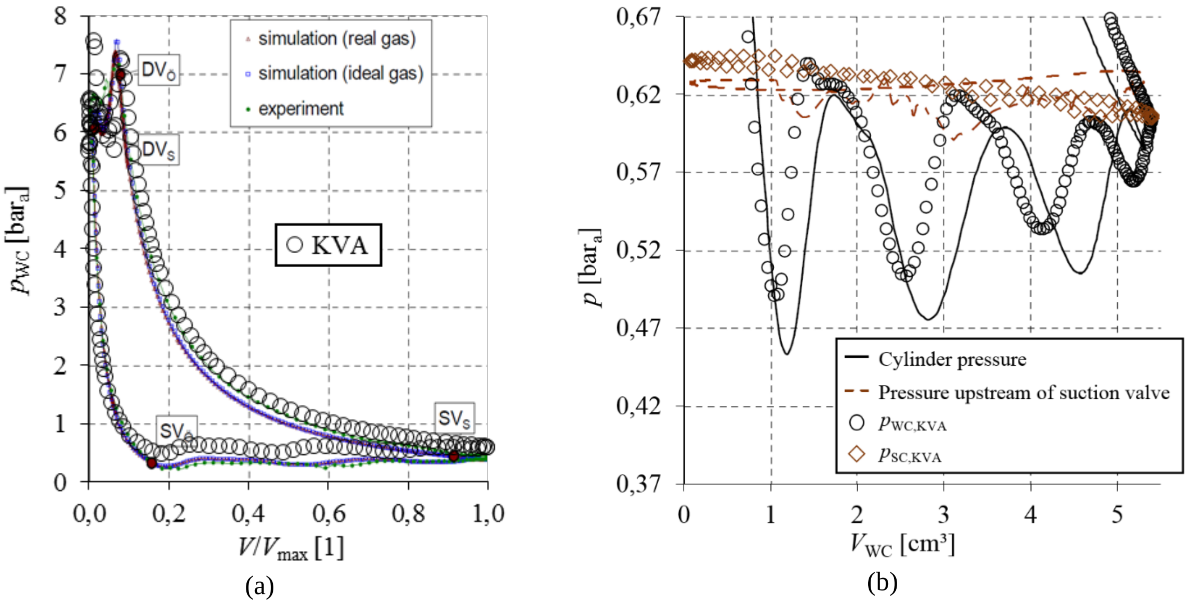


**Figure 3**: Comparison of $p$,$V$ diagrams (a) and the pressure curves for the intake period (b) (see Lang (2010) for original diagrams)

Figure 3 (a) shows the change of the thermodynamic state within the compressor working chamber based on the experimental results from Lang (2010) (dotted measurement points) and based on the KVA calculation results (circles). The KVA calculation results are similar to the experimental data particularly regarding the trend of both compression and re-expansion curve. The characteristic pressure curves as shown in Figure 3 (b) are a result of the valve oscillation during inflow and outflow. The calculated valve behavior shows an acceptable agreement with the suction chamber pressure curve (dashed line and diamond symbols) and the working chamber pressure curve (solid line and circles). Figure 4 shows the valve lift of both suction and discharge valve. The KVA calculation results satisfactorily represent the experimental suction valve behavior. The pressure curve and the valve lift curve for the discharge valve show deviations that are acceptable within the scope of this calculation approach.

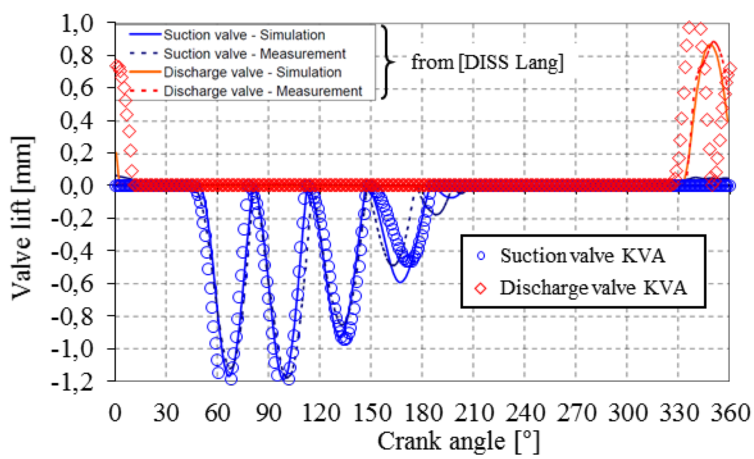


**Figure 4**: Comparison of KVA valve lift results and experimental/simulation data of Lang (2010)

This graphical comparison shows the applicability of the KVA calculation model. KVA can be used to reliably derive operating parameters such as the internal power or the valve behavior with less computational effort compared to more detailed simulations. Table 1 lists essential experimentally derived compressor parameters and the corresponding KVA calculation results.

**Table 1:** Comparison of relevant parameters of the reciprocating compressor from Lang (2010) and KVA (KVA results only include internal losses)

| Parameter | Symbol | Unit | Lang (2010) | KVA |
|---|---|---|---|---|
| Electrical power | $P_{el}$ | [W] | 57.42 | 52.40 |
| Mass flow | $\dot{m}$ | [g s$^{-1}$] | 0.275 | 0.283 |

## 4. MODELLING AND CALCULATION OF A WANKEL COMPRESSOR

### 4.1 KVA Model for a 2:3 Wankel compressor design

KVA was further used to test the suitability of a Wankel compressor as a refrigerator compressor. The cylinder part of a 2:3 rotary compressor (whose housing is a two-lobed epitrochoid) was selected and designed for the same operating point and speed as the reciprocating compressor. The mathematical description of Nash (1977) is used for the basic geometry of both cylinder and displacer. The selected parameters $R_b$ (radius of basic circle for epitrochoid construction), $R_r$ (radius of rolling circle for epitrochoid construction) and $H$ (height of Wankel displacer, set to 17.4 mm) lead to a mass flow rate that approximately corresponds to the reciprocating compressor (see Figure 10 (a)). The positioning of both inlet and outlet ports was based on a favorable resulting process control. The selected geometry is shown in Figure 5 (a).

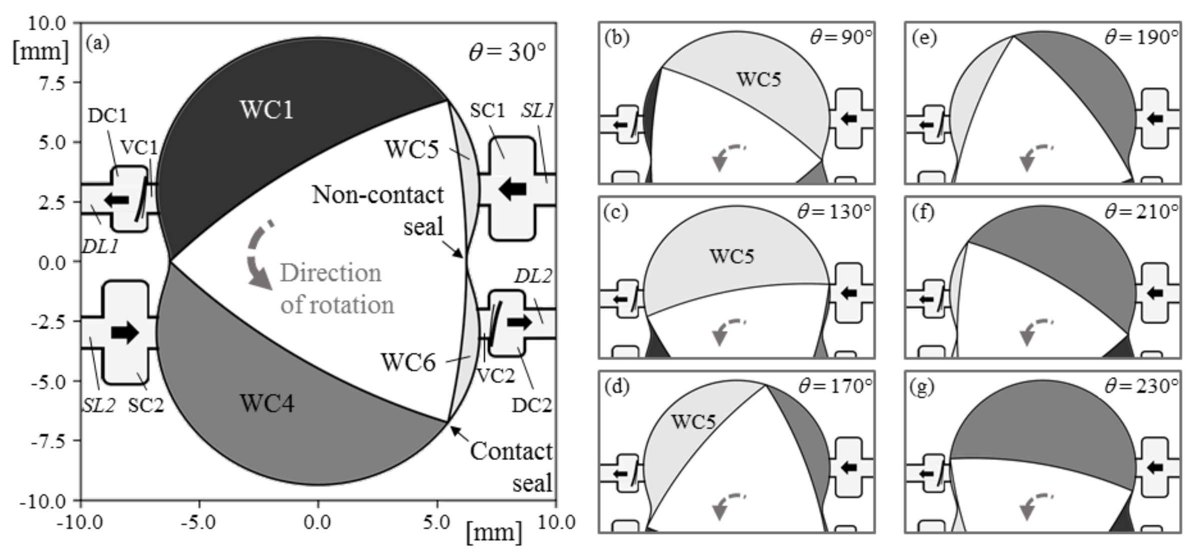


**Figure 5**: Cylinder and displacer geometry of the Wankel compressor (a) and suction, compression and discharge process for the working chamber 5 (b) - (g)

Figures 5 (b)–(g) show the compression process for the working chamber 5. The compression process consists of the suction (b)-(c), the compression (c)-(f) and the discharge (f)-(g) of the refrigerant. These processes happen within each working chamber, which is formed by the cylinder (axial and radial boundaries) and the respective displacement flank as well as the contact seal at the displacer edges. There is one compression process per revolution for each working chamber. The offset between neighboring chamber processes (*e.g.* WC1 and WC4) is 120° which results from the design of the displacer. This results in six complete compression processes for one revolution of the displacer. This may lead to a smoother gas flow compared to reciprocating compressors. Further a Wankel compressor does not require a crank drive and but comprises a gearing mechanism between the cam and the displacer (not shown in Figure 5) which leads to a more compact design compared to reciprocating compressors.

A 2:3-type trochoid compressor shows a special behavior during the compression process. The compressed gas is partially separated from the discharge port when the displacement flank approaches the cylinder cusp (non-contact seal in Figure 5). The gas in this separated chamber cannot be pushed through the discharge port as the displacer continues to rotate. After the separation, the compressed gas expands until the separated chamber is connected to the suction port and thus behaves similarly to a clearance volume of a reciprocating compressor. The KVA model considers the separation of the working chamber and the leakage between the separated chambers (*e.g.* WC5 and WC6) at the cylinder cusp. Figure 6 shows the resulting chamber volume curves for the given geometric specifications. A volume of zero means that the chamber does currently not exist (*e.g.* the working chambers WC4 and WC5 as well as WC1 and WC2 have the same volume at a displacer angle of 90°, whereas the chambers WC3 and WC6 do not exist at this point). The corresponding KVA calculation model for the Wankel compressor is shown in Figure 7.

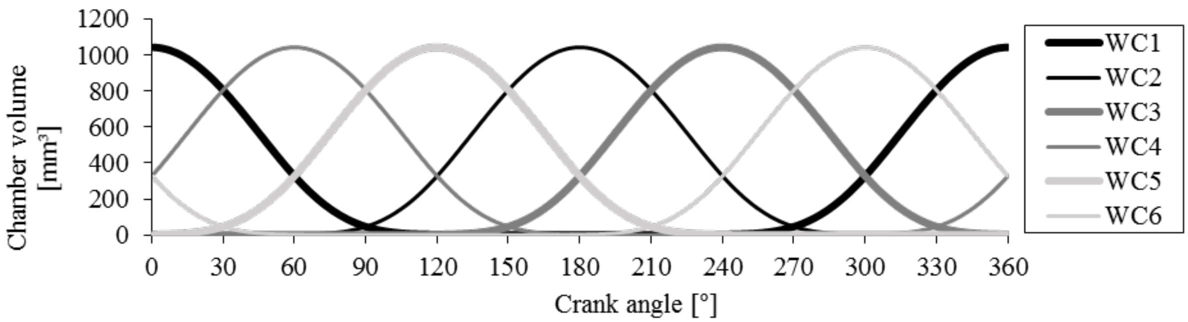


**Figure 6**: $V, \theta$ diagram of each compression chamber during one displacer revolution

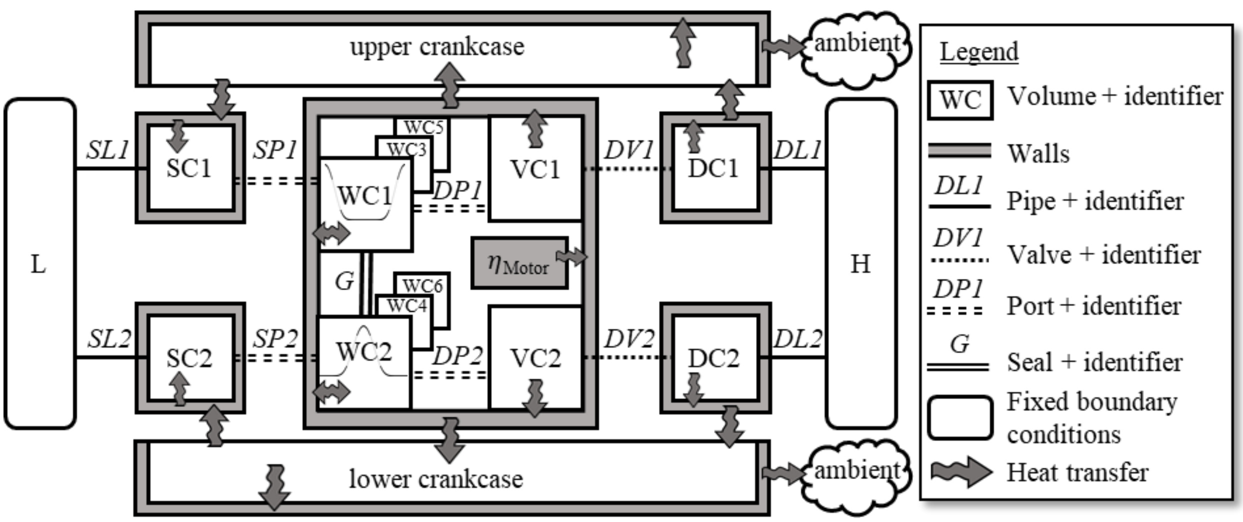


**Figure 7**: Structure of the KVA Wankel compressor model

The thermodynamic state is similar to the HTK model and the boundary conditions are given by the fixed low-pressure and high-pressure side (L, H). The two-lobed shape of the cylinder leads to two separate but similarly designed flow paths in the Wankel model. Each flow path consists of a suction line (*SL1*, *SL2*) which leads to a suction chamber (SC1, SC2). The connections between the suction chambers and working chambers are modeled as suction ports (*SP1*, *SP2*) due to process reasons. In a 2:3 Wankel machine there are a maximum of six distinguishable working chambers (WC1 – WC6, see Figure 5 and 6) and a maximum of four working chambers exist simultaneously. All six working chambers are modeled with time-dependent volumes corresponding to the curves shown in Figure 6. The working chambers are connected to the suction lines via time-dependent cross-sections corresponding to the edges of the inlet ports (see Figure 5 (a)). The special features of an edge-controlled suction flow are therefore considered. Each outlet port (*DP1*, *DP2*) is connected to the active working chamber. The working chambers and the high-pressure side are connected via discharge valves. However, the discharge valves cannot be positioned directly on the inner cylinder circumference (see Figure 5) which leads to separate valve nests that are modeled as separate volumes (VC1, VC2) prior to the discharge valve. The working chambers and the valve nests are located within the cylinder block and they are surrounded by a common wall. The gap between two working spaces (*G*) is modelled as a non-contact leak between the cylinder cusp and the moving displacement flank. The model further includes the high-pressure chambers (DC1, DC2) and pressure lines (*DL1*, *DL2*) after the discharge valves. All elements are assumed to be within the compressor housing and are therefore thermally connected to the gas-filled chambers (upper and lower crankcase). The compressor housing transfers heat to the environment.

### 4.2 Comparison of calculation results of reciprocating and Wankel compressor

The two KVA models for the reciprocating and Wankel compressor were used to calculate the compressor performance for the operating point specified in Lang (2010). The thermodynamic boundary conditions (suction temperature, low and high pressure, ambient temperature) and the compressor speed were the same for both calculations. The chosen Wankel compressor dimensions lead to a mass flow similar to the one of the reciprocating compressor (see geometry in Figure 5 (a)), the height of the displacer is 17.4 mm). Figure 8 shows the resulting *p*,*V* diagram of both compressor types.

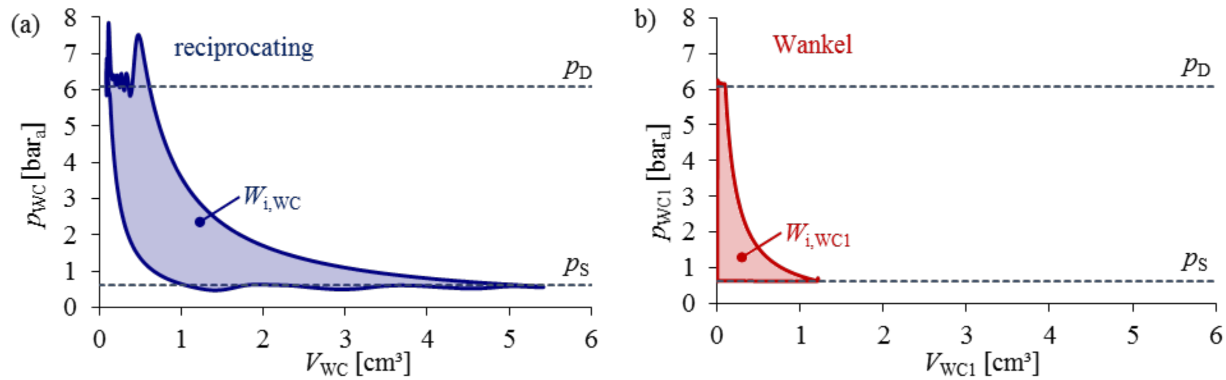


**Figure 8**: Comparison of *p*,*V* diagrams from KVA calculations of the reciprocating compressor (a) and of one working chamber (WC1) of the Wankel compressor (b)

Both *p*,*V* diagrams differ significantly in the size or their enclosed area which refers to their indicated work $W_i$. The Wankel compressor delivers approximately the same mass flow as the reciprocating compressor, but it also has six compression cycles at one full rotation of the displacer which leads to a smaller displacement of each working chamber. In addition, the Wankel compressor has no re-expansion phase, which is clearly visible in the reciprocating compressor *p*,*V* diagram and leads to a reduced maximum geometric intake volume and a lower volumetric efficiency. The duration of the suction phase is similar for both compressors (the inlet is opened for 130° of the displacer angle ~7.3 ms), but the Wankel compressor shows less pressure pulsations due to its edge-controlled operation without suction valves. The discharge process of the Wankel compressor is advantageous as well since only one-sixth of the mass must be discharged as compared to the reciprocating compressor. Further the dimensions of the discharge valve are less limited within the Wankel cylinder which leads to lower pressure pulsations and flow pressure losses during discharge.

Figure 9 shows the calculations results for the pressure in both suction and discharge chamber. The results of the Wankel compressor show less fluctuations in the high- and low-pressure side which may be an indicator for the more uniform and continuous operation as compared to the reciprocating compressor. The pressure pulsations of the reciprocating compressor are usually damped by a muffler and buffer vessels on the suction- and the high-pressure side, respectively. The size of these damping components may be reduced in the case of a Wankel compressor or may be omitted completely.

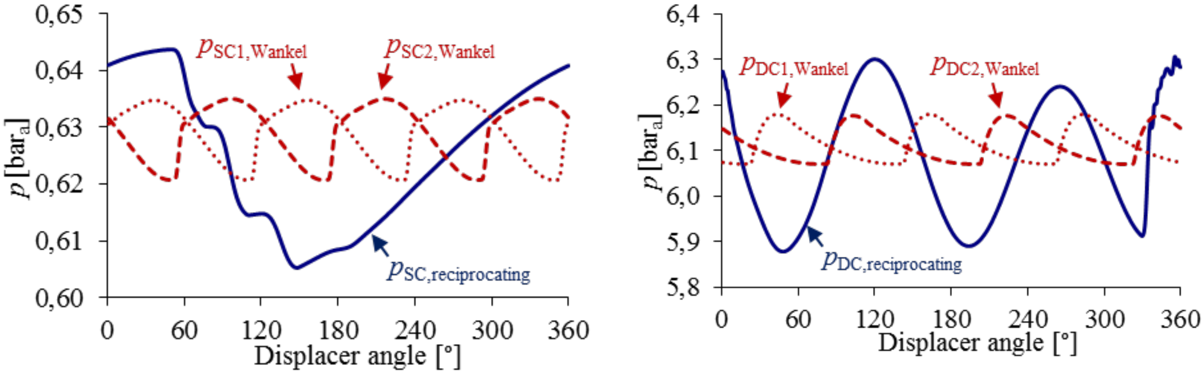


**Figure 9**: Comparison of the KVA results for the pressure curves from the suction (a) and discharge chambers (b) of the reciprocating and the Wankel compressor

Another important result is the leakage of both compressors. The internal leakage of the Wankel compressor is one of the major loss factors regarding the efficiency of this compression principle. The calculation results of the Wankel compressor reveal a great influence of the gaps between the displacement flanks and the cylinder cusps. The authors assumed a constant gap width of 1 µm for the KVA Wankel calculation model. This rather small gap would be very difficult to achieve in a real machine and presumably overestimates the efficiency of the Wankel compressor in the present calculation. The average leakage during one complete displacer rotation is 0.03 g $s^{-1}$ and it flows from the working chamber upstream of the high-pressure valve to the working chamber downstream of the inlet. This mass flow loss is compensated by the larger displacement volume of the Wankel compressor design. The displacement volumes of all working chambers of the rotary compressor (each approx. 1.22 $cm^3$ (see Figure 6) per compression process) add up to a displacement of approx. 7.3 $cm^3$ per displacer revolution which exceeds the displacement of the reciprocating compressor (see Figure 8 (a)). Furthermore, the internal leakage also reduces the Wankel compressor's efficiency. This impact is greater than the reciprocating compressor's re-expansion which mainly reduces the volumetric efficiency. The overall performance parameters are shown in Figure 10. The mass flow was the target value and is therefore approximately the same for the measurements from Lang (2010) and the KVA calculations for both compressor types. However, the total indicated power of the reciprocating compressor is considerably lower than with the Wankel compressor which leads to a significantly higher energy efficiency (see isentropic efficiency).

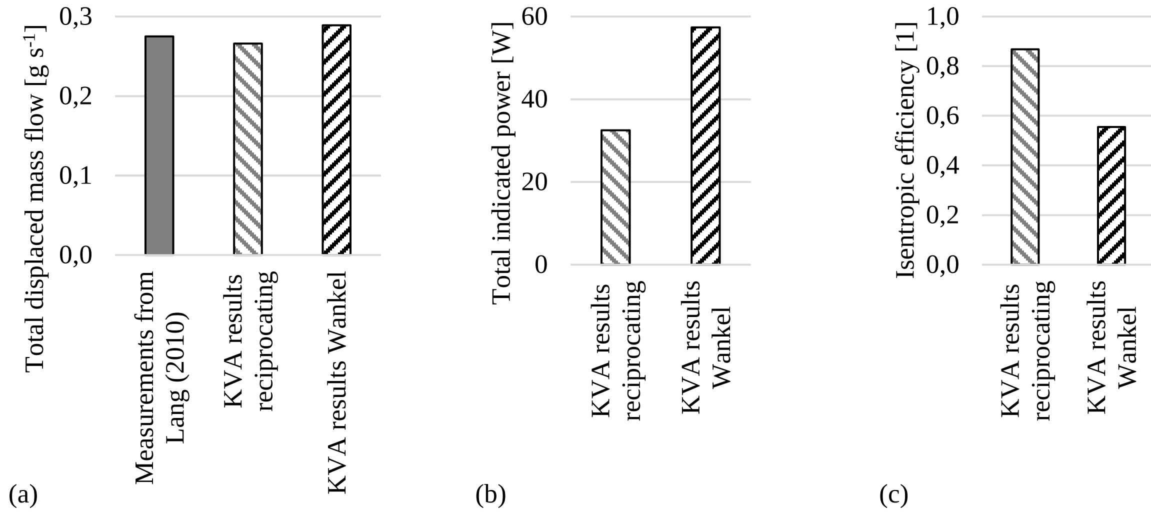


**Figure 10**: Comparison of the total displaced mass flow (a), the total indicated power (b) and the isentropic efficiency (c) of the reciprocating and Wankel compressor

## 5. CONCLUSION

The compressor calculation software KVA has been successfully tested for small scale compressors. The results of the KVA model for the household refrigerator compressor ACC HTK55 AA are in good agreement with the available experimental data. The KVA calculation results for the Wankel compressor design confirm Wankel compressor benefits as mentioned in related publications. The results show reduced pressure pulsations for the Wankel compressor as compared to the reciprocating compressor. Further the calculation shows no negative effect of any dead volume and the re-expansion is negligible compared to the reciprocation compressor. The lack of pulsation dampers, a more compact driving mechanism and the smaller working chambers may lead to a more compact compressor design. However, the results also show a lower isentropic efficiency of the Wankel compressor. This is mainly caused by increased internal leakages at the non-contact sealing gaps at the cylinder cusps. The Wankel type compressor seems to be less convenient for the pressure ratio of a household refrigerator compressor. The comparatively low displaced mass flow requires a high production quality (*e.g.* tolerances) to effectively reduce internal leakage. The manufacturability of the miniature driving mechanism should also be considered within the considered capacity range. The Wankel compressor is currently not competitive with the typical reciprocating compressors in domestic refrigeration systems.

## NOMENCLATURE

| | | |
|---|---|---|
| $e$ | specific exergy | (J kg$^{-1}$) |
| $H$ | height of Wankel displacer | (m) |
| HTC | heat transfer coefficient(s) | (W m$^{-2}$ K$^{-1}$) |
| $h_\mathrm{v}$ | valve lift | (m) |
| $h$ | specific enthalpy | (J kg$^{-1}$ K$^{-1}$) |
| $K$ | isentropic exponent factor | (1) |
| $l_\mathrm{v}$ | valve perimeter | (m) |
| $m$ | mass | (kg) |
| $\dot{m}$, $\dot{m}_j$ | mass flow | (kg s$^{-1}$) |
| $Nu$ | Nusselt number | (1) |
| $p$ | pressure | (bar$_\mathrm{a}$) |
| $P_\mathrm{el}$ | electrical power | (W) |
| $Pr$ | Prandtl number | (1) |
| $Q$ | heat | (J) |
| $R$ | specific gas constant | (J kg$^{-1}$ K$^{-1}$) |
| $R_\mathrm{b}$ | radius of basic circle for epitrochoid construction | (m) |
| $R_\mathrm{r}$ | radius of rolling circle for epitrochoid construction | (m) |
| $Re$ | Reynolds number | (1) |
| $s$ | specific entropy | (J kg$^{-1}$ K$^{-1}$) |
| $t$ | time | (s) |
| $T$ | temperature | (K) |
| $V$ | volume | (m$^3$) |
| $W_{\mathrm{i,WC}}$, $W_{\mathrm{i,WC1}}$ | indicated power of a working chamber | (J) |
| $\alpha_\mathrm{flow}$ | flow coefficient of valve | (1) |
| $\theta$ | displacer angle | (°) |
| $\varrho$ | density | (kg m$^{-1}$) |
| $\varphi$ | crank angle | (°) |
| $\psi_\mathrm{f}$ | force coefficient of valve | (1) |

**Subscript**

| | |
|---|---|
| KVA | compressor system (german: Kolbenverdichteranlage) |
| max | maximum |
| SC | suction chamber |
| WC, WC1 | working chamber, working chamber 1 |

## REFERENCES

Antonelli, M., Francesconi, M., Baccioli, A., & Caposciutti, G. (2017). *Experimental results of a Wankel-type expander fuelled by compressed air and saturated steam*. Energy Procedia, 105, 2929-2934.

Garside, D. W. (2017). *A new Wankel-type compressor and vacuum pump*. In IOP Conference Series: Materials Science and Engineering (Vol. 232, No. 1, p. 012065). IOP Publishing.

Hesse, U., & Will, G. (2014). *Thermodynamic Calculation of Reciprocating Compressors Plants*. Proceedings of the 9th Conference of the EFRC, Vienna, Austria (158-168).

Kaiser, H., & Kruse, H. (1984). *An Investigation on Reciprocating and Rotary Refrigeration Compressors*. International Compressor Engineering Conference. Paper 508. http://docs.lib.purdue.edu/icec/508

Lang, W. (2010). *Erstellung von Simulationsmodellen für ausgewählte Problemstellungen bei der Entwicklung von hermetischen Kolbenkompressoren*, PhD thesis, Graz University of Technology.

Nash, D. H. (1977). *Rotary Engine Geometry*. Mathematics Magazine, 50(2), 87-89.

Ogura, I. (1982). *The Ogura-Wankel compressor-Application of Wankel Rotary Concept as Automotive Air Conditioning Compressor* (No. 820159). SAE Technical Paper.

Surek, D., & Stempin, S. (2014). *Technische Strömungsmechanik.* Wiesbaden, Germany: Springer Vieweg

Wrede, F., & Kruse, H. (1986). *Recent status of trochoidal type compressors for heat pumps in Germany. International Compressor Engineering Conference*. Paper 530. http://docs.lib.purdue.edu/icec/530

Wu, Y. T., Ma, C. F., & Zhong, X. H. (2010). Development and experimental investigation of a miniature-scale refrigeration system. *Energy Conversion and Management*, *51*(1), 81-88.